# Molecular Mechanics Simulations on Covalent Complexes of Mitomycin C and Its Analogues with Left-Handed DNA Duplexes

Shashidhar N. Rao,*,† Bhashyam S. Iyengar,‡ Timothy P. Wunz,‡ and William A. Remers‡

*Searle Research and Development, Division of G.D. Searle and Company, 4901 Searle Parkway, Skokie, Illinois 60077, and College of Pharmacy, University of Arizona, Tucson, Arizona 85721.* *Received February 19, 1991*

We present molecular mechanics simulations on covalent complexes between d(GCGCGCGCGC)·d(GCGCGCGCGC) in the left-handed double helical forms (B and Z) and potent antitumor antibiotics mitomycin C and three of its analogues using the all atom force field in the framework of the program AMBER(UCSF). The energy-refined models of the complexes show interesting networks of hydrogen-bonding interactions between the drugs and DNA groups in the minor groove of the left-handed helices. The energy-refined models suggest that mitomycins could bind strongly to left-handed helices. This result might be relevant to the interpretation of earlier experiments which suggested that DNA bound by mitomycin C underwent a transition to a non-Z left-handed structure.[1]

## Introduction

Mitomycin C is a potent, clinically useful antitumor agent that covalently binds to individual DNA strands and cross-links the complementary strands of a duplex DNA. The nature of its covalent interactions with DNA and the structure of the resultant complex have been the subject of a number of investigations in recent years.[2] Recent experiments have shown the predominant interacting mode of mitomycins[3-5] to be through minor-groove alkylation, with N2 (the exocyclic amino nitrogen) of guanine being the alkylating site on DNA. There is further evidence for this mode of binding from recent biochemical experiments which demonstrate a modulation of mitomycin cross-linking caused by DNA bending induced from the binding of CAP protein to DNA.[6]

In three publications from our laboratories,[7-9] we have reported model-building and energy-minimization studies on the covalent and noncovalent complexes between mitomycin C and its derivatives on one hand and a variety of DNA duplexes on the other. Similar studies have also been recently reported by Arora et al. in which aspects of orientational preferences of the mitomycins in the major and minor grooves have been addressed.[10] The modeled structures were consistent with the observations derived from physicochemical experiments and demonstrated good qualitative correlationship between the calculated net binding energies of the drugs to DNA and their biological potencies.

To date, the literature on DNA–mitomycin interactions has emphasized the binding of the drug to the right-handed polymorphic form of DNA. Since minor-groove alkylation is the predominant mode of mitomycin interaction with DNA, it is important to understand if the drug could bind to the well-characterized minor-groove structures in the left-handed double-helical forms such as left-handed Z-DNA (LZ)[11] and left-handed uniform B-DNA (LB).[12] The left-handed Z-DNA has been implicated in a number of biologically important processes.[13] An understanding of these potential interactions may be significant in the interpretation of $^{31}P$ NMR and radioimmunoassay studies on DNA–mitomycin complexes, which together with CD studies predicted a DNA transition from a right-handed B form to a left-handed non-Z conformation.[1]

In this light, we have undertaken molecular modeling studies on the monocovalent complexes between mitomycin C (MC, 1) and three of its derivatives, mitomycin A (MA, 2), M83 (3), and BMY-25282 (BMY, 4) (Figure 1),

**Scheme I.** Bioreductive Activation and DNA Binding by Mitomycin C

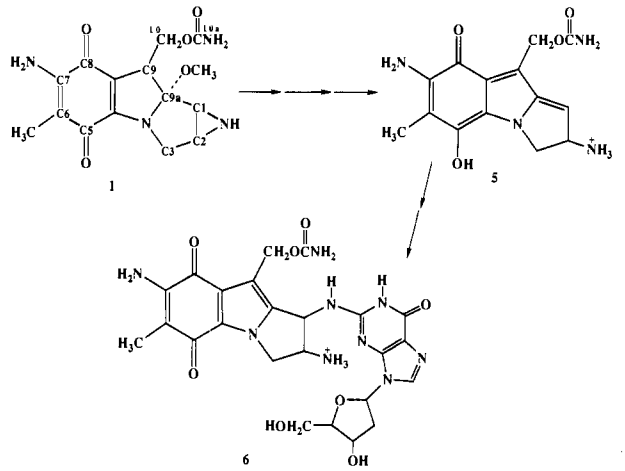

and left-handed DNA in the B and Z forms to understand the nature of drug–DNA interactions. We chose the sequence d(GCGCGCGCGC)·d(GCGCGCGCGC), abbreviated GC10, since poly(dG-dC)·poly(dG-dC) is known to adopt both B and Z forms under varying experimental conditions (see ref 14 and references therein). We have

* To whom correspondence should be addressed.
† Searle Research and Development.
‡ University of Arizona.

(1) Tomasz, M.; Barton, J. K.; Magliozzo, C.; Tucker, D.; Lafer, E. M.; Stollas, B. D. *Proc. Natl. Acad. Sci. U.S.A.* **1983**, *80*, 2874–2878.
(2) Remers, W. A.; Dorr, R. T. Chemisry, biology and therapeutics of mitomycins. *Alkaloids: Chem. Biol. Prospect.* **1988**, *6*, 1–74.
(3) Tomasz, M.; Lipman, R.; Verdine, G.; Nakanishi, K. *Biochemistry* **1986**, *25*, 4337.
(4) Tomasz, M.; Chowdary, D.; Lipman, R.; Shimotokahara, D.; Veiro, D.; Walker, V.; Verdine, G. L. *Proc. Natl. Acad. Sci. U.S.A.* **1986**, *83*, 6702.
(5) Tomasz, M.; Lipman, R.; Chowdary, D.; Pawlak, J.; Verdine, G. L.; Nakanishi, K. *Science* **1987**, *235*, 1204.
(6) Cera, C.; Crothers, D. M. *Biochemistry* **1989**, *28*, 3908–3911.
(7) Rao, S. N.; Singh, U. C.; Kollman, P. A. *J. Am. Chem. Soc.* **1986**, *108*, 2058.
(8) Remers, W. A.; Rao, S. N.; Singh, U. C.; Kollman, P. A. *J. Med. Chem.* **1986**, *29*, 1256.
(9) Remers, W. A.; Rao, S. N.; Wunz, T. P.; Kollman, P. A. *J. Med. Chem.* **1988**, *31*, 1612.
(10) Arora, S. K.; Cox, M. B.; Arjunan, P. *J. Med. Chem.* **1990**, *33*, 3000–3008.
(11) Wang, A. H.-J.; Quigley, G. J.; Kolpak, F. J.; van der Marel, G. A.; van Boom, J. H.; Rich, A. *Science* **1981**, *211*, 171–176.
(12) Gupta, G.; Bansal, M.; Sasisekharan, V. *Int. J. Biol. Macromol.* **1980**, *2*, 368.
(13) Wells, R. D.; Amirhaeri, S.; Blaho, J. A.; Collier, D. A.; Hanvey, J. C.; Hsieh, W.-T.; Jaworski, A.; Klysik, J.; Larson, J. E.; McLean, M. J.; Wohlrab, F.; Zacharias, W. In *Unusual DNA Structures*. Wells, R. D., Harvey, S. C., Eds.; Springer-Verlag: New York, 1988; pp 1–21.

0022-2623/91/1834-3380$02.50/0 

**Table I.** Energy Components in the Complexes between GC10 in Right-Handed B (RB), Left-Handed B (LB), and Left-Handed Z (LZ) and Mitomycins

| DNA | total | intermolecular | | | intramolecular | | | | | | |
|---|---|---|---|---|---|---|---|---|---|---|---|
| | | elec[a] | vdw | $E_{d\text{-}h}$[b] | Hel1[c] | Hel2[d] | $E_{dis}$[e] | $E_{d1}$[f] | $E_{d2}$[g] | $E_{dd}$[h] | $E_{netb}$[i] |
| | | | | | Mitomycin C | | | | | | |
| RB | −895.2 | −101.2 | −28.3 | −116.3 | −792.8 | −812.0 | 19.2 | 5.0 | −4.3 | 9.3 | −87.8 |
| LB | −838.7 | −98.1 | −22.8 | −118.1 | −741.3 | −749.4 | 8.1 | 10.0 | −4.3 | 14.3 | −95.7 |
| LZ | −815.9 | −178.2 | −18.7 | −188.6 | −638.4 | −691.1 | 52.7 | 2.4 | −4.3 | 6.7 | −129.2 |
| | | | | | Mitomycin A | | | | | | |
| RB | −890.7 | −94.6 | −29.1 | −110.5 | −795.2 | −812.0 | 16.8 | 6.1 | −2.4 | 8.5 | −85.2 |
| LB | −834.3 | −91.8 | −22.8 | −111.6 | −740.8 | −749.4 | 8.6 | 7.3 | −2.4 | 9.7 | −93.3 |
| LZ | −816.3 | −164.8 | −21.0 | −177.8 | −648.6 | −691.1 | 42.5 | 4.0 | −2.4 | 6.4 | −128.9 |
| | | | | | M83 | | | | | | |
| RB | −882.7 | −138.8 | −21.0 | −159.1 | −794.8 | −812.0 | 17.2 | 18.7 | −18.7 | 37.4 | −104.5 |
| LB | −836.7 | −147.1 | −10.8 | −157.9 | −721.7 | −753.4 | 31.7 | −10.2 | −18.7 | 8.5 | −117.7 |
| LZ | −850.0 | −202.9 | −13.0 | −215.9 | −692.2 | −729.7 | 37.5 | 1.8 | −18.7 | 20.5 | −157.9 |
| | | | | | BMY-25282 | | | | | | |
| RB | −916.2 | −184.9 | −13.5 | −198.4 | −792.4 | −812.0 | 19.6 | 24.7 | 14.2 | 10.5 | −168.3 |
| LB | −885.7 | −222.1 | −12.3 | −232.4 | −727.5 | −753.4 | 25.9 | 23.8 | 14.2 | 9.6 | −196.9 |
| LZ | −870.7 | −272.5 | −01.7 | −274.2 | −679.5 | −717.6 | 38.1 | 27.9 | 14.2 | 13.7 | −222.4 |

[a] In the AMBER force field, the electrostatic component of hydrogen bonds is evaluated as a normal Coulombic interaction with distance-dependent dielectric constant and is included with the electrostatic energy term. The steric component of hydrogen-bonding interaction is evaluated through a 10–12 van der Waals term, which accounts for only a small portion of the total hydrogen bonding interactions (±0.6 kcal/mol). Both the components are included in the electrostatic part of the interaction energy. [b] Total intermolecular energy. [c] Energy of the helix in the complex. [d] Energy of the helix minimized from the complex with the drug removed. [e] Helix-distortion energy. [f] Energy of the drug in the complex. [g] Energy of the drug alone. [h] Drug-distortion energy. [i] Net binding energy ($E_{d\text{-}h} + E_{dis} + E_{dd}$).

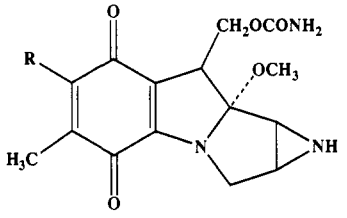


**MC** R = $NH_2$

**MA** R = $OCH_3$

**M83** R = $NHC_6H_4OH$

**BMY** R = $NHCH=\overset{+}{N}(CH_3)_2$

**Figure 1.** Structures of mitomycin C and three of its derivatives.

also carried out simulations on the complexes with right-handed B-DNA (RB) to make meaningful comparisons with the left-handed models. Our earlier simulations[7-9] on these complexes were done in the framework of the united atom force field, while the present study is being done in the framework of the all atom force field.

The covalent binding of mitomycins to DNA takes place by a process of bioreductive activation in which the mitomycin is converted into a reactive intermediate that alkylates the 2-amino group of a guanosine residue.[3] As shown in abbreviated form in Scheme I, the quinone ring of mitomycin C (1) is reduced to a hydroquinone that loses the elements of methanol from the 9- and 9a-positions. Protonation of the aziridine nitrogen results in ring opening with the formation of a reactive intermediate (5).[15] The 2-amino group adds to the conjugated carbonyl system of this intermediate. The resulting adduct is reoxidized to quinone 6. This quinone is used in our modeling studies.

Comparisons with our earlier proposed models based on right-handed B-DNA show that the left-handed complexes are stereochemically feasible just as the former and that there is no overwhelming energetic preference in favor of the former to rule out complex formation with left-handed DNA structures. The results are indicative of a possible inducement of conformational transitions between the right and left-handed polymorphs of DNA. Our results will hopefully inspire further experiments using high-resolution X-ray crystallography and solution techniques such as 2D NMR/NOE under varying physicochemical conditions.

## Results and Discussion

Figure 2 is a schematic for the polynucleotide–drug complexes in this study. Stereo views of energy-refined complexes of the four mitomycins with right-handed B-DNA and left-handed B- and Z-DNA are presented in Figures 3–5, respectively. The energy components (see Experimental Section) and hydrogen-bonding parameters in the left- and right-handed complexes are presented in Tables I and II, respectively. As in earlier investigations, we present individual interactions between the drugs on one hand and DNA constituents on the other in Table III. In this study, as in our earlier studies on DNA–mitomycin complexes, the conformational changes are confined to predominantly the sugar puckerings and phosphodiester bond rotations. These are not detailed here, but the relevant data is available upon request from the authors.

The RB complexes are very similar in their characteristics (drug–DNA interactions and conformational variations in the nucleotide backbone) to those obtained earlier with the united atom force field[7] and hence are not discussed in detail. However, the data on their component energetics and hydrogen-bonding interactions are presented in the appropriate tables.

All the energy-refined complexes with the left-handed duplexes share common and interesting conformational features. The overall helix distortions are minimal and conformational disturbances in the structures are confined to regions in the site of covalent adduct formation. In both the LB and LZ complexes of MC and MA, the drugs lie entirely inside the deep minor groove and are held together

(14) Rao, S. N.; Jovin, T.; Kollman, P. A. In *Unusual DNA Structures*. Wells, R. D., Harvey, S. C., Eds.; Springer-Verlag: New York, 1988; pp 267–285.
(15) Moore, H. W. *Science* **1964**, *145*, 55.

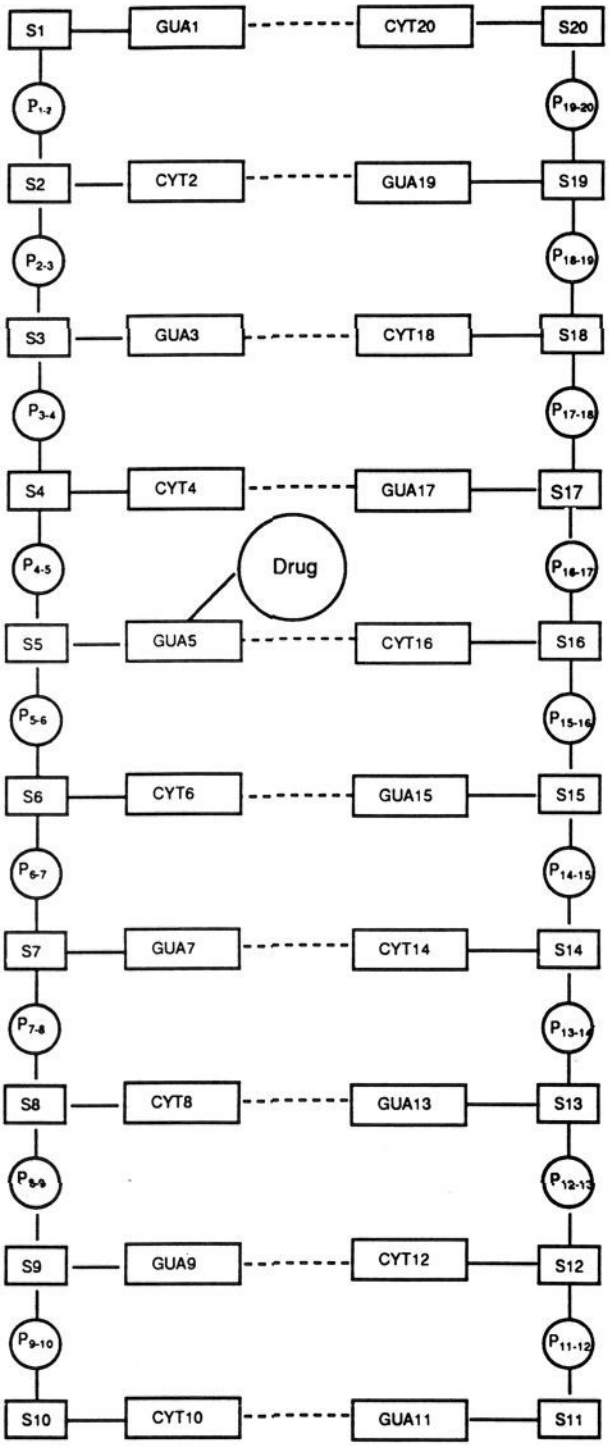


**Figure 2.** Schematic for decanucleotide duplexes. S stands for sugar. Nucleotides are numbered as GUA1, CYT2, etc., with the numbering continuing into the complementary strand as GUA11, CYT12, etc. The phosphate groups are referred to as $P_{n-m}$ where $n$ and $m$ are the nucleotides on the 5′- and 3′-sides.

by strong hydrogen-bonding interactions with the sugar–phosphate backbone of the oligonucleotide. In all the LB complexes, the distance of the C10 in the drugs to the N2 in GUA17 is around 3.2 Å, which is just around the sum of the van der Waals radii of carbon and nitrogen in the AMBER force field. This suggests the possibility of their cross-linking the complementary strands.

In the complex between M83 and left-handed B-DNA (LB–M83) and in the complex between BMY and left-handed B-DNA (LB–BMY), the substituents on the amino group at C-7 lie almost entirely outside the double helix in a solvent-exposed fashion. In fact, in contrast to the models with RB, the phenolic hydroxyl is not hydrogen

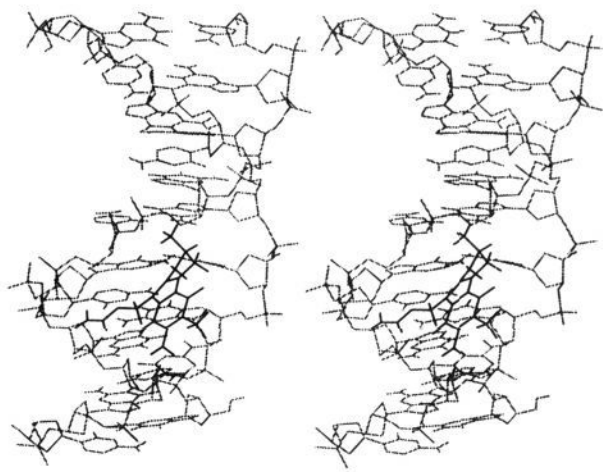

**Figure 3.** Stereo pair for RB–MC.

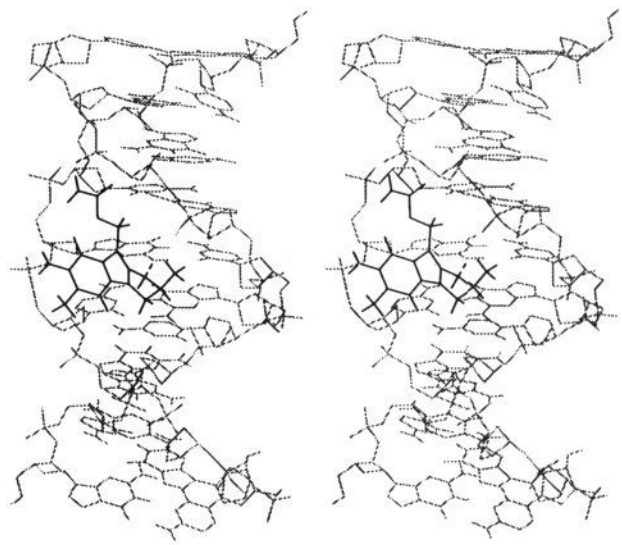

**Figure 4.** Stereo pair for LB–MC.

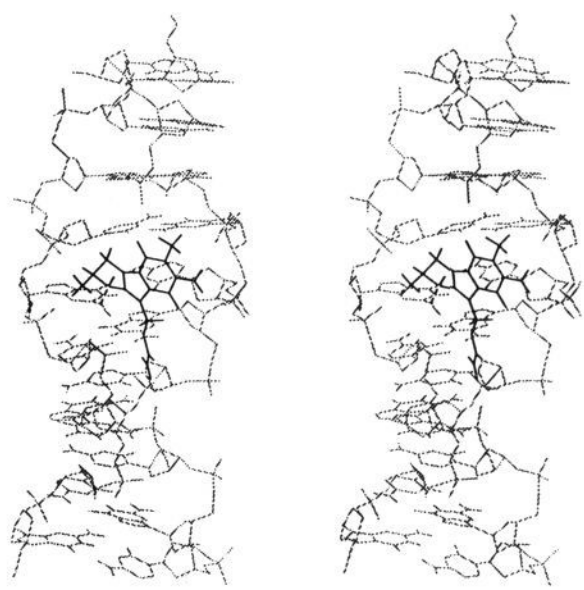

**Figure 5.** Stereo pair for LZ–MC.

**Table II.** Hydrogen-Bonding Parameters Involving Interactions of GC10 in LB, RB, and LZ Forms in Their Complexes with MC, MA, M83, and BMY

| complex | donor (X–H) | acceptor atom (Z) | length, Å | angle, deg |
|---|---|---|---|---|
| RB–M83 | N3–HN3A(M83) | O3′(CYT6) | 2.07 | 159.3 |
| | N3–HN3B(M83) | O2(CYT6) | 1.77 | 155.0 |
| | N3–HN3C(M83) | O1′(GUA7) | 1.73 | 166.7 |
| | N1–HN1B(M83) | OB($P_{17-18}$) | 1.81 | 172.3 |
| | O6–HO6(M83) | OB($P_{18-19}$) | 1.69 | 161.8 |
| | N2–HN2B(GUA17) | O5(M83) | 1.88 | 155.6 |
| LB–M83 | N3–HN3A(M83) | O5(M83) | 1.73 | 157.2 |
| | N3–HN3B(M83) | N3(GUA17) | 1.84 | 154.6 |
| | N3–HN3C(M83) | O3′(GUA17) | 2.20 | 127.2 |
| | N4–HN41(M83) | O3′(CYT18) | 1.87 | 145.4 |
| | N4–HN42(M83) | OB($P_{19-20}$) | 2.01 | 121.5 |
| | N2–HN2B(GUA17) | O5(M83) | 1.87 | 155.1 |
| LZ–M83 | N3–HN3B(M83) | OA($P_{5-6}$) | 1.64 | 154.2 |
| | N3–HN3C(M83) | OA($P_{4-5}$) | 1.64 | 152.5 |
| | N4–HN41(M83) | OA($P_{7-8}$) | 1.67 | 173.3 |
| | N4–HN42(M83) | OA($P_{6-7}$) | 1.69 | 160.5 |
| | O6–HO6(M83) | OA($P_{16-17}$) | 1.64 | 171.1 |
| RB–BMY | N3–HN3B(BMY) | O2(CYT6) | 1.75 | 156.8 |
| | N3–HN3C(BMY) | O1′(GUA7) | 1.75 | 160.0 |
| | N1–HN1B(BMY) | OB($P_{17-18}$) | 1.61 | 160.1 |
| | N2–HN2B(GUA17) | O5(BMY) | 1.85 | 156.5 |
| LB–BMY | N4–HN42(BMY) | O3′(CYT18) | 1.85 | 166.5 |
| | N3–HN3B(BMY) | N3(GUA17) | 1.77 | 155.7 |
| | N3–HN3C(BMY) | O3′(GUA17) | 1.72 | 175.9 |
| LB–BMY | N1–HN1B(BMY) | OB($P_{5-6}$) | 1.63 | 153.8 |
| | N2–HN2B(GUA17) | O3(BMY) | 1.98 | 136.8 |
| LZ–BMY | N3–HN3B(BMY) | OA($P_{5-6}$) | 1.68 | 137.7 |
| | N3–HN3C(BMY) | OA($P_{4-5}$) | 1.64 | 155.6 |
| | N4–HN41(BMY) | OA($P_{7-8}$) | 1.67 | 172.9 |
| | N4–HN42(BMY) | OA($P_{6-7}$) | 1.68 | 164.4 |
| | N1–HN1B(BMY) | OA($P_{16-17}$) | 1.65 | 140.3 |
| RB–MC | N3–HN3B(MC) | O2(CYT6) | 1.72 | 167.6 |
| | N3–HN3C(MC) | O1′(GUA7) | 2.03 | 152.5 |
| | N1–HN1B(MC) | OB($P_{17-18}$) | 2.18 | 123.1 |
| | N2–HN2B(GUA17) | O5(MC) | 2.07 | 154.7 |
| LB–MC | N3–HN3B(MC) | O2(CYT16) | 1.68 | 167.4 |
| | N1–HN1A(MC) | OB($P_{5-6}$) | 2.08 | 126.4 |
| | N2–HN2B(GUA17) | O5(MC) | 2.20 | 155.1 |
| | N4–HN41(MC) | OB($P_{4-5}$) | 2.00 | 136.0 |
| LZ–MC | N3–HN3B(MC) | OA($P_{5-6}$) | 1.65 | 139.2 |
| | N3–HN3C(MC) | OA($P_{4-5}$) | 1.64 | 154.0 |
| | N4–HN41(MC) | OA($P_{7-8}$) | 1.94 | 168.9 |
| | N4–HN42(MC) | OA($P_{6-7}$) | 1.98 | 160.6 |
| | N1–HN1A(MC) | OA($P_{16-17}$) | 1.99 | 153.7 |
| | N1–HN1B(MC) | OA($P_{17-18}$) | 2.10 | 161.2 |
| RB–MA | N3–HN3B(MA) | O2(CYT6) | 1.71 | 167.2 |
| | N3–HN3C(MA) | O1′(GUA7) | 2.02 | 155.8 |
| | N2–HN2B(GUA17) | O5(MA) | 2.11 | 152.0 |
| LB–MA | N3–HN3B(MA) | O2(CYT16) | 1.68 | 169.2 |
| | N2–HN2B(GUA17) | O5(MA) | 2.14 | 126.9 |
| | N4–HN41(MA) | OB($P_{4-5}$) | 2.00 | 137.0 |
| LZ–MA | N3–HN3B(MA) | OA($P_{5-6}$) | 1.65 | 139.2 |
| | N3–HN3C(MA) | OA($P_{4-5}$) | 1.64 | 154.0 |
| | N4–HN41(MA) | OA($P_{7-8}$) | 1.94 | 168.9 |
| | N4–HN42(MA) | OA($P_{6-7}$) | 1.98 | 160.6 |

[a] In a hydrogen bond X–H···Z, X and Z are respectively the donor and the acceptor atoms. The hydrogen bond length corresponds to the distance between H and Z, while the angle is X–H···Z.

bonded to any constituent of the oligonucleotide backbone and is solvent exposed. However, in the corresponding models with left-handed Z-DNA, LZ–M83 and LZ–BMY, the same substituents are partially inside the minor groove of the double helix. In fact, the phenolic hydroxyl in M83 of LZ–M83 lies almost entirely inside the minor groove, being hydrogen bonded to a pendant oxygen of $P_{16-17}$. The observed helix-shape-dependent disposition of the substituents on the C-7 of mitomycin analogues could have an impact on the effective contributions of solvation to their overall binding.

In all the LZ complexes, two of the protons on N2 of the drugs are hydrogen bonded to pendant oxygens on $P_{4-5}$ and $P_{5-6}$ while the amino group protons in the carbamate side chain are hydrogen bonded to the pendant oxygens on $P_{6-7}$ and $P_{7-8}$. None of the carbamoyloxy groups on the drugs are involved in any directed hydrogen-bonding interactions with DNA constituents. For example, O5 is pointed toward the floor of the minor groove in all the LZ complexes. The corresponding C=O group is generally oriented toward the exocyclic amino groups of the neighboring guanine residues, with which they may form water-bridged hydrogen bonds in solution. The quinone C=O groups are nonspecifically oriented in the minor groove. This scenario of the carbamoyloxy groups is in sharp contrast to the models with B form of duplexes, where they are involved in directed hydrogen bonds. The NH group at C-7 in LZ–BMY is hydrogen bonded to $P_{16-17}$ while the

**Table III.** Energies (kcal/mol) of Interactions between MA, MC, M83, and BMY and DNA Components in Their Covalent Complexes for RB, LB, and LZ Polymorphic Forms

| | M83 | | | BMY | | | | mitomycin A | | | mitomycin C | | |
|---|---|---|---|---|---|---|---|---|---|---|---|---|---|
| DNA group | RB | LB | LZ | RB | LB | LZ | DNA group | RB | LB | LZ | RB | LB | LZ |
| $P_{3-4}$ | | | -8.2 | | -4.6 | -7.7 | $P_{3-4}$ | | | -5.3 | | | -5.4 |
| CYT4 | | | -5.5 | | | -4.4 | GUA3 | | -4.0 | | | -4.1 | |
| $P_{4-5}$ | | -5.3 | -64.2 | -5.2 | -12.6 | -52.7 | $P_{4-5}$ | -3.2 | -13.3 | -48.1 | -3.0 | -13.2 | -47.9 |
| GUA5 | -14.0 | -8.1 | -22.0 | -20.0 | -23.6 | -15.1 | $P_{5-6}$ | -10.4 | -8.9 | -44.1 | -9.8 | -16.1 | -43.9 |
| $P_{5-6}$ | -6.1 | | -37.8 | -9.2 | -40.0 | -37.0 | $P_{6-7}$ | -23.2 | -12.6 | -20.9 | -23.7 | -13.7 | -20.1 |
| CYT12 | -19.1 | -4.6 | -5.0 | -16.1 | | | $P_{7-8}$ | -7.8 | -5.8 | -12.9 | -7.7 | -5.6 | -12.6 |
| $P_{6-7}$ | -40.4 | -13.6 | -25.2 | -27.3 | -13.4 | -38.1 | $P_{8-9}$ | -3.1 | | | -3.1 | | |
| $P_{7-8}$ | -11.7 | -4.5 | -17.1 | -11.0 | -5.4 | -24.3 | $P_{14-15}$ | | -3.0 | | | -3.0 | |
| CYT25 | -9.4 | -9.8 | -6.4 | -7.4 | -6.7 | -6.3 | $P_{15-16}$ | -3.9 | -6.3 | | -3.9 | -6.2 | |
| GUA28 | -8.7 | -15.8 | | -9.1 | -15.2 | | $P_{16-17}$ | -7.0 | -11.6 | -7.2 | -7.1 | -11.6 | -13.5 |
| $P_{14-15}$ | | | | | | -4.7 | GUA15 | | | -3.0 | | | (-2.7) |
| $P_{16-17}$ | -10.2 | -10.6 | -15.6 | -12.2 | -10.3 | -51.0 | GUA17 | -6.8 | -5.0 | | -7.0 | -4.8 | |
| $P_{17-18}$ | -9.8 | -57.2 | -5.5 | -55.3 | -43.7 | -28.3 | $P_{17-18}$ | -11.7 | -10.9 | -10.5 | -18.9 | -10.4 | -18.5 |
| $P_{18-19}$ | -12.8 | -25.3 | -9.8 | -19.1 | -51.0 | -12.2 | $P_{18-19}$ | -3.0 | -5.4 | -9.0 | -3.0 | -3.8 | -9.1 |

corresponding group in LZ–M83 is pointed toward the solvent exposed surface, away from the floor of the minor groove. As pointed out earlier, $P_{16-17}$ binds to the phenolic hydroxyl in this complex. In LZ–MC, the C-7 amino group is hydrogen bonded to $P_{16-17}$ and $P_{17-18}$ while such interactions are absent in LZ–MA.

In LB–M83 and LB–BMY, one of the three protons on C-2 ammonium is hydrogen bonded to N3 of GUA17, while another is hydrogen bonded to O3′ of the same residue. In LZ–M83 and LZ–BMY, the C-2 ammonium is hydrogen bonded to the O2 of CYT16. The other two hydrogens of this group are located deep inside the minor groove but are not bonded to any of the nucleotide groups. This contrasts with the situation in the right-handed complexes, where the ammonium is strongly hydrogen bonded with a negatively charged phosphate group in the strand containing alkylated guanine.

The oligonucleotide components in the LB complexes of mitomycins C and A are very nearly identical in structure and conformation. As is to be expected, the only major difference in the interaction profiles of the drug with DNA relates to the substitution at C-7. While the amino group in MC is hydrogen bonded to $P_{5-6}$, the methoxy group in MA is inclined to the quinone ring and is disposed on the surface of the minor groove. Similar differences are also seen in the models of MC and MA complexed to the right-handed DNA.

The carbonyl group in the mitomycin side chain has different environments in different LB complexes. In LB–BMY, O5 is hydrogen bonded to the exocyclic amino group of GUA3, while in LB–M83, this atom is hydrogen bonded to the protonated ammonium at C-2 and the exocyclic amino group of GUA17. The protons in both these guanine residues are the ones not involved in Watson–Crick pairing with their complementary cytosines. In the other two LB complexes, O5 is electrostatically sandwiched between the exocyclic amino groups of GUA3 and GUA17. The distances between O5 and the protons of these amino groups (2.2 to 2.6 Å) are a little longer than necessary for the formation of strong hydrogen bonds.

One of the protons in the amino group of the carbamate side chain is hydrogen bonded to $P_{4-5}$ in LB–MC and LB–MA, while the other proton is weakly hydrogen bonded to O5′ of GUA5. In the other two complexes, one of the carbamate NH groups is hydrogen bonded with the O3′ of CYT18, while the other is hydrogen bonded to $P_{18-19}$ in LB–M83 and is oriented toward N3 of GUA19 and O2 of CYT18 in LB–BMY.

Table I lists the energetics of the energy-refined structures. Total, intermolecular (elec, vdw, and $E_{d-h}$), intramolecular (Hel1, Hel2, $E_{dis}$, $E_{d1}$, $E_{d2}$, and $E_{ddis}$), and net binding energies $E_{netb}$ (in kcal/mol) are defined and tabulated. The energies of isolated helices (Hel2) were determined by starting with the minimized drug–DNA complexes, removing the drug, replacing the hydrogen on the 2-amino group of GUA5, and reminimizing the energy. Such minima were obtained separately for RB-, LB- and LZ-DNA. The lowest value obtained for a particular helix is used in the table for comparison with all drug–DNA complexes containing this helix. The helix-distortion energy is the energy of the helix in a complex (Hel1) minus the energy of the isolated helix (Hel2). Drug-distortion energy is the energy of the drug in a complex minus the energy of the minimized isolated drug. For all the four drugs, the energies of the isolated and minimized drugs, starting from their structures in the complexes, are almost identical (within 0.1 kcal/mol).

For all four drug–DNA complexes investigated, the net binding energies are most favored in the case of Z-DNA complexes. The LB complexes have net drug–DNA interaction favored over the RB complexes in the case of BMY and M83. In the Z-DNA complexes, the helix distortions are found to be generally larger than those in RB and LB complexes.

In light of the above discussed conformational features, it is clear that the dominant contribution to the net drug–DNA interactions arises from electrostatic interactions, particularly in the left-handed complexes. These contributions cover ranges extending up to 90 kcal/mol while the van der Waals component of the interactions are spread over a narrower range of 8–12 kcal/mol. The latter component is most favored in the complexes with right-handed DNA. The drug-distortion energies for BMY range from 9.6 to 13.7 kcal/mol. BMY is most distorted in its LZ complex, while MC and MA are most distorted in their LB complexes, probably to accommodate the most favored electrostatic and hydrogen-bonding interactions with DNA constituents. The distortion energies of M83 are, in contrast, highest in the complexes with RB-DNA (Table I).

The helix distortions in LB complexes of MC and MA are around 8 kcal/mol. The similarity in helix distortions is reflected in the similarity of the corresponding complexes. In RB complexes, the helix distortions are somewhat larger for mitomycin C, BMY, and M83 than for mitomycin A. This probably could be attributed to the fact the first three drugs are more tightly bound to the DNA helix, and in order to maximize their interactions with DNA, the helix may be distorted marginally higher than in the complex with MA. The helix distortions are considerably larger for Z-DNA complexes, and for reasons similar to those in the right-handed B form of DNA, the distortions in the case of MC are higher than in the case

**Table IV.** Base-Stacking Interactions in the Complexes between Mitomycins and Right- and Left-Handed DNA Duplexes and Base Pair Interaction Energies for the GUA5-CYT16 Base Pair

| stacked bases | mitomycin A | | | mitomycin C | | |
|---|---|---|---|---|---|---|
| | RB | LB | LZ | RB | LB | LZ |
| GUA3-CYT4 | −10.2 | −8.6 | −9.5 | −10.2 | −8.6 | −9.6 |
| CYT4-GUA5 | −6.2 | −6.7 | −2.7 | −6.2 | −6.7 | −2.4 |
| GUA5-CYT6 | −8.6 | −5.2 | −11.2 | −8.5 | −5.4 | −11.6 |
| CYT6-GUA7 | −2.7 | −6.4 | −6.3 | −2.6 | −6.3 | −5.6 |
| CYT14-GUA15 | −7.5 | −7.2 | −6.5 | −7.5 | −7.3 | −6.2 |
| GUA15-CYT16 | −8.6 | −6.5 | −6.6 | −8.5 | −6.6 | −5.4 |
| CYT16-GUA17 | −6.1 | −7.5 | −4.5 | −6.1 | −7.4 | −4.7 |
| GUA17-CYT18 | −10.2 | −8.1 | −9.6 | −10.3 | −8.1 | −9.1 |
| stacked bases | M83 | | | BMY | | |
| | RB | LB | LZ | RB | LB | LZ |
| GUA3-CYT4 | −9.0 | −7.0 | −8.3 | −9.0 | −7.8 | −8.4 |
| CYT4-GUA5 | −4.9 | −4.0 | −1.5 | −4.7 | −4.6 | −0.7 |
| GUA5-CYT6 | −4.6 | −3.3 | −2.9 | −3.8 | −3.4 | −6.8 |
| CYT6-GUA7 | −2.5 | −5.9 | −4.2 | −2.9 | −6.0 | −5.1 |
| CYT14-GUA15 | −6.7 | −6.4 | −5.0 | −6.7 | −6.5 | −4.7 |
| GUA15-CYT16 | −9.5 | −7.6 | −3.7 | −9.0 | −8.1 | −5.9 |
| CYT16-GUA17 | −5.7 | −5.6 | −5.1 | −5.5 | −4.8 | −3.2 |
| GUA17-CYT18 | −9.1 | −7.7 | −9.3 | −9.2 | −7.9 | −8.7 |

| | GUA5-CYT16 interaction energies | | | | GUA5-CYT16 interaction energies | | |
|---|---|---|---|---|---|---|---|
| | RB | LB | LZ | | RB | LB | LZ |
| MC | −20.9 | −21.0 | −10.6 | M83 | −15.9 | −12.1 | −13.8 |
| MA | −21.0 | −21.0 | −11.1 | BMY | −14.7 | −13.5 | −9.2 |

of MA by more than 10 kcal/mol.

The net binding energies of MC, M83, and BMY follow a common relative trend (being the largest for BMY and smallest for MC), irrespective of DNA polymorphism. In an earlier investigation, we had shown that the binding energies of the three compounds were qualitatively consistent with the effective doses required.[9] We find that such a consistency is also observed for models with the left-handed duplexes LB and LZ. The net binding energies for MA are very close to those of MC. This is not surprising in the light of the similarities in their complexes. However, this similarity in the net binding energies is not qualitatively fully consistent with their relative potencies of MC and MA, and this could be due to a number of other factors not accounted for in this investigation.

Table III lists the energies of interactions between the drugs on one hand and the DNA constituents (bases and phosphates) on the other. Only the interactions whose magnitudes are greater than 3.0 kcal/mol are listed. The profiles in these interactions correspond to the geometric features listed in Table II.

In all the complexes none of the base pairs is distorted significantly from the Watson–Crick configuration, with the exception of the CYT16-GUA5 pair. Base pairing interaction energies are around −22 kcal/mol for all the pairs except for the CYT16-GUA5 pair, where they vary from −9 to −16 kcal/mol in the complexes with M83 and BMY (Table IV) and from −10.6 to −21 kcal/mol in the complexes with MA and MC. Interestingly, in the complexes with both the right- and left-handed B-DNA duplex, mitomycin C and mitomycin A produce distortions of only about 1 kcal/mol for the base pair involving the covalently linked guanine. The loss of about 6 to 13 kcal/mol for this pair in the rest of the complexes could be attributed to changes in the base-pairing geometries brought by the constraints of covalent linkage of the drugs with the exocyclic amino group of GUA5.

As pointed out earlier, the overall helix distortions are generally small. In the case of RB complexes, the calculated helix energies (Table I) are practically identical for the four drugs. This is consistent with the corresponding energy components (total base interactions, sugar–phosphate backbone interactions, and backbone–base interactions) of the isolated helices as listed in Table V. In LB complexes, the total energies of the isolated helices vary from −749.4 kcal/mol (MC and MA) to −753.4 kcal/mol (BMY and M83). The latter two helices have slightly favored base–backone and sugar–phosphate interactions (Table V). By contrast to the LB and RB complexes, the helix energies in LZ complexes vary over a wider range (−691.1 kcal/mol in LZ–MC and LZ–MA to −729.7 kcal/mol in LZ–M83). The principal cause of this variation seems to be set of interactions involving the sugar–phosphate backbone, since the total base–base interactions are very similar in all the four LZ complexes. The base–backbone and sugar–phosphate interactions are significantly favored in the BMY and M83 complexes (Table V) compared to the other two complexes. This could be possibly attributed to different disposition profiles for

**Table V.** Energies (in kcal/mol) of Bases and Sugar–Phosphate Backbone and Base–Backbone Interactions in GC10 Structures Obtained by Refinement of the Oligonucleotide Part from the Drug–DNA Complexes

| complex | bases[a] | sugar–phosphate backbone interactions | base–backbone interactions |
|---|---|---|---|
| RB–MC | −812.9 | 46.6 | −45.1 |
| RB–MA | −813.0 | 46.4 | −45.1 |
| RB–M83 | −815.7 | 44.2 | −43.8 |
| RB–BMY | −813.3 | 46.8 | −45.1 |
| LB–MC | −795.5 | 104.0 | −57.8 |
| LB–MA | −795.6 | 104.5 | −58.0 |
| LB–M83 | −792.4 | 101.8 | −62.7 |
| LB–BMY | −792.9 | 103.2 | −63.2 |
| LZ–MC | −780.9 | 116.0 | −26.1 |
| LZ–MA | −780.0 | 116.4 | −26.4 |
| LZ–M83 | −775.4 | 89.7 | −43.8 |
| LZ–BMY | −776.2 | 101.8 | −43.1 |

[a] Includes energies of base-stacking, base-pairing, and cross-base interactions for all the ten base pairs of GC10. [b] Includes sugar–sugar and phosphate–phosphate repulsion and sugar–phosphate interaction energies for all the ten nucleotide pairs in GC10. [c] Includes energies of interactions between all the bases and all the sugars and energies of interactions between all the bases and all the phosphates in GC10.

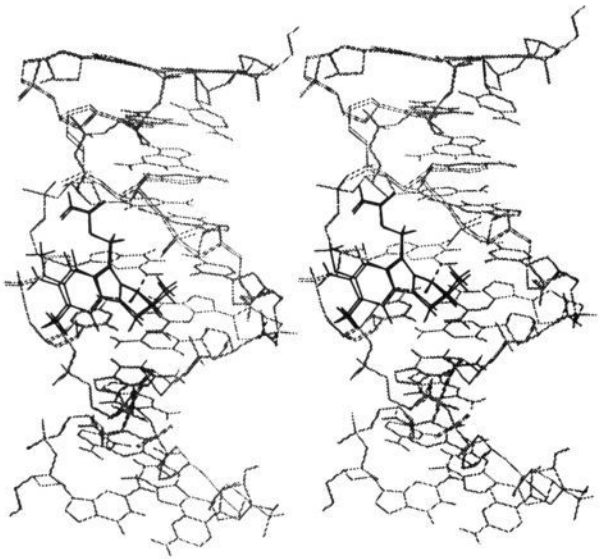

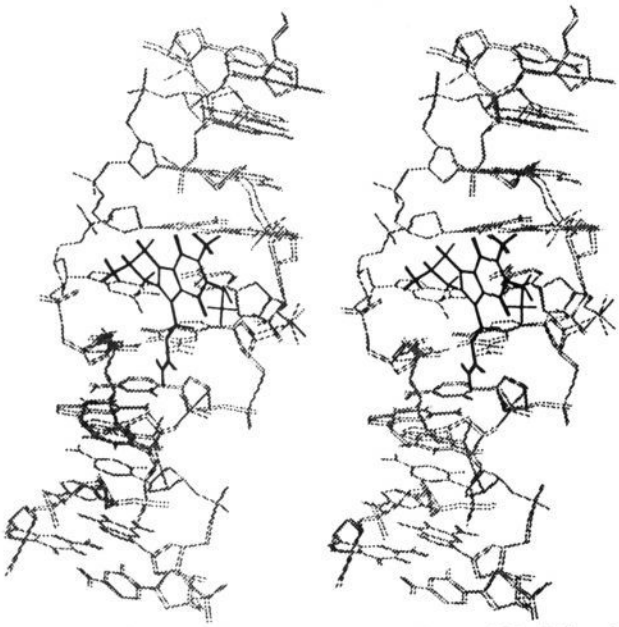

**Figure 6.** Stereo pairs for the superposition of LB–MC and LB–MA (a) and LZ–MC and LZ–MA (b).

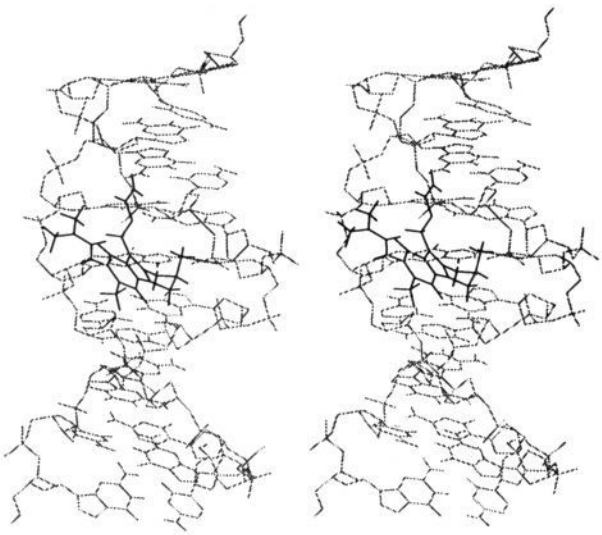

**Figure 7.** Stereo pair for LB–BMY.

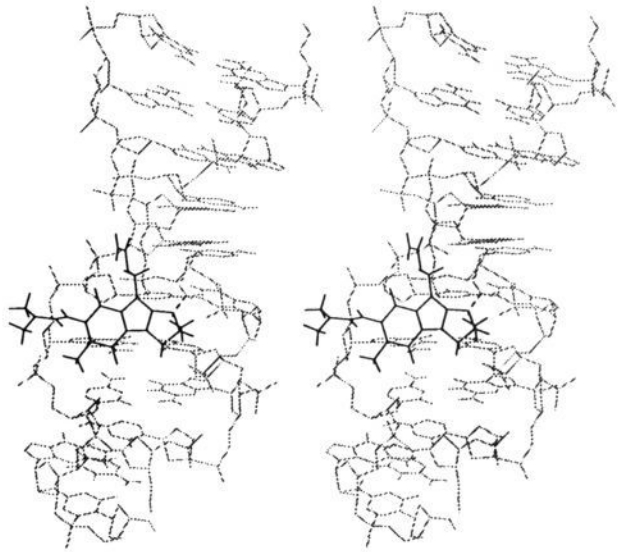

**Figure 8.** Stereo pair for LZ–BMY.

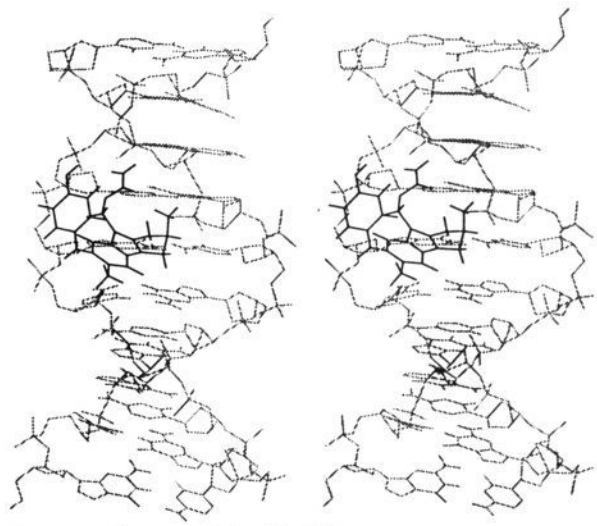

**Figure 9.** Stereo pair for LB–M83.

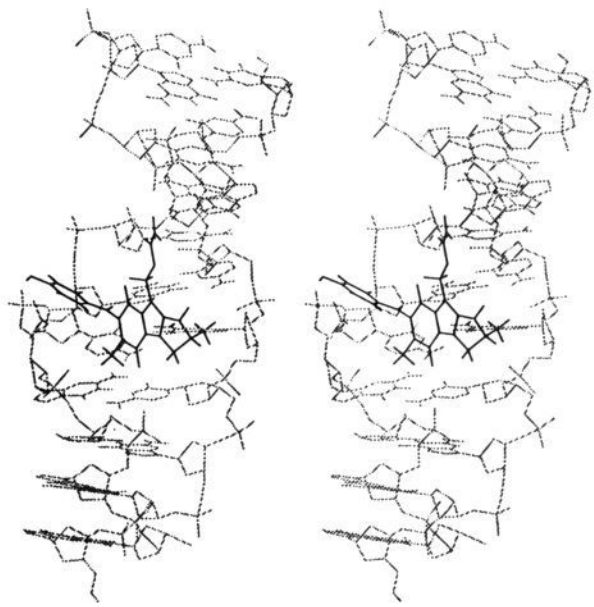

**Figure 10.** Stereo pair for LZ–M83.

these two drugs with respect to the sugar–phosphate backbone (Figures 8 and 10) compared to the profiles of MC and MA (Figure 6b).

To the best of our knowledge, this is the first study to investigate models of a groove-binding drug complexed with a left-handed uniform duplex like LB-DNA. These models provide geometrical insights into possible alternative modes for mitomycins binding to DNA. While no solution studies have yet "found" a left-handed B-DNA structure, X-ray fiber diffraction and model-building studies have demonstrated that stereochemically feasible models of LB-DNA satisfy the fiber data as well as right-handed duplex structures do.[12]

It must be emphasized that the molecular mechanics approach employed in this investigation does not give a quantitative analysis of the free energies of interactions of mitomycins and their analogues to various polymorphic forms of DNA or the energetics for the reaction pathway for covalent binding. The calculated total energies do not have explicit representation of solvation and counterion effects. In addition, the electrostatics are treated through the simple Coulombic potential with a distance-dependent dielectric (see Experimental Section) leading to possible overemphasis of electrostatic stabilization of the complexes. Although the calculations predict an overwhelming binding preference of mitomycins to left-handed Z-DNA, in light of the above mentioned simplicity of treatment of electrostatic effects, their relative binding to right-handed DNA cannot be deemphasized. Nevertheless, the calculated models provide useful qualitative insights into the binding of mitomycins to various DNA forms. On the basis of the fact that the present calculations do not rule out binding to left-handed forms of DNA, molecular dynamics simulations with explicit inclusion of solvent and counterions have been initiated on the right- and left-handed complexes. Such studies are likely to provide further insights into the relationship between binding modes of drugs and nucleic acid polymorphism.

Prior to the revision of binding mode of mitomycins to the predominantly minor-groove alkylation,[3-5] they were considered to bind predominantly in the major groove.[16-18] In such a light, results of $^{31}P$ NMR experiments were interpreted in terms of a transition of the DNA to a non-Z left-handed structure from the canonical B form.[1] The present investigations have addressed the question of binding of mitomycins to the left-handed polymorphic forms of DNA and have shown that the binding of the drugs to left-handed forms (either B or Z) cannot be ruled out on enthalpic considerations alone. The wider minor grooves in the left-handed DNA duplexes seem to be at least equally good binding pockets as the minor groove of the right-handed B-DNA.

## Conclusions

All atom molecular mechanics investigations have been carried out on monocovalent alkylation complexes of DNA in left- and right-handed double helical forms with mitomycin C and three of its derivatives. The drugs are bound in the minor groove and interact with the proximal DNA residues through a network of hydrogen bonds. The right-handed B-DNA complexes obtained with the united atom and all atom force fields had practically identical structures. The previously observed qualitative consistency[9] for the relative biological potencies of mitomycin C, M83, and BMY is also seen for models with left-handed B and Z forms of DNA. The studies are suggestive of possibilities of mitomycins alkylating left-handed forms of DNA. Our results provide valuable insights into the interpretation of high-resolution 2D-NMR and X-ray crystallographic studies on DNA–mitomycin complexes.

## Experimental Section

The nomenclature for the drug atoms and the various residues of the decanucleotide is the same as earlier.[7-9] The starting structures of the complexes between the DNA decamers and mitomycins were obtained through computer graphics molecular model building (using MIDAS[19]) as described earlier.[7-9] The starting coordinates for LZ-DNA were obtained from the published crystal structure of a Z-DNA hexamer[11] and those for LB-DNA were obtained from the model based on the fiber diffraction studies of nucleic acids.[12] The starting structures for all the four drugs were based on the crystal structure of 1-*N*-(*p*-bromobenzoyl)-mitomycin C.[20]

The model-built structures were energy minimized in two stages using the molecular mechanics package AMBER(UCSF)[21] and the all atom force field parameters presented by Weiner et al. (1986).[22] In the first stage, only the drug was allowed to move. In the following stage, all the degrees of freedom were allowed to move. This procedure was adopted to ensure that no unwanted distortions, possibly emanating due to the limitations in the hand-docking procedures, were set into the left-handed DNA structures.

The parameters and partial atomic charges for the drug molecules were evaluated in the framework of the all atom force field. The charges for the mitomycin derivatives were obtained, as earlier,[7-9] from quantum chemically derived electrostatic potentials calculated using STO-3G basis set in GAUSSIAN80-UCSF,[23] fully consistent with the AMBER force field for nucleic acids.[22] New atom types and other parameters for mitomycins A and C were reported previously.[7] No new parameters were required for the phenol substituent of M83. It was necessary, however, to define new atom type (CV) for the carbon atom in the center of the amidinium ion substituent of protonated BMY-25282. Force field parameters for bonds and angles involving CV were taken from AMBER parameters for the protonated histidine residue (HN–CV–NH)$^+$. The torsional parameter X–CV–N–X was set at a barrier of $V/2 = 5.8$ kcal/mol deg to emphasize coplanarity of the amidinium ion. These force field parameters are given in the supplementary material (Table VI).

All the nonbonded interactions were evaluated. A distance-dependent dielectric constant was used and all the simulations were done in vacuum without any explicit solvent or counterions. In all the complexes, the drug orientation is the same as in our earlier models with right-handed B-DNA.[7,9]

As earlier, we have carried out component analyses of energies of interactions in order to estimate the relative energetic stabilities of various complexes. To compare the relative binding interactions for a drug with different polynucleotides, the net binding energies are used. They are calculated by subtracting the helix-distortion and drug-distortion energies from the total drug–DNA interaction energy. These distortion energies reflect induced fits that permit stronger intermolecular interactions. Drug and helix distortion energies are obtained by subtracting the energies of the drug or helix, obtained after they are separated from the complexes and

(16) Szybalski, W.; Iyer, V. N. In *Antibiotics I. Mechanism of Action*, Gottlieb, D., Shaw, P. D., Eds.; Springer-Verlag: New York, 1967; 211–245.
(17) Tomasz, M.; Mercado, C. M.; Olson, N.; Chatterjee, N. *Biochemistry* **1974**, *13*, 4878.
(18) Hashimoto, Y.; Shudo, K.; Okamoto, T. *Tetrahedron Lett.* **1982**, *23*, 667.
(19) Ferrin, T. E.; Huang, C. C.; Jarvis, L. E.; Langridge, R. *J. Mol. Graph.* **1988**, *6*, 1–27.
(20) Shirahata, K.; Hirayama, N. *J. Am. Chem. Soc.* **1983**, *105*, 7199–7200.
(21) Singh, U. C.; Weiner, P. K.; Caldwell, J. W.; Kollman, P. A. AMBER(UCSF), version 3.0; Department of Pharmaceutical Chemistry, University of California, San Francisco, CA 94143, 1986.
(22) Weiner, S. J.; Kollman, P. A.; Nguyen, D.; Case, D. *J. Comput. Chem.* **1986**, *7*, 230–252.
(23) Singh, U. C.; Kollman, P. A. *J. Comput. Chem.* **1984**, *5*, 129–144.

reminimized, from their energies in the complexes. In addition, we have evaluated the energies of interaction between the drugs and nucleotide residues (sugars, phosphates, and bases) located close to them. These are schematically illustrated in Figure 2.

**Acknowledgment.** We thank the Drug Design Group of Searle Research and Development for the computational facilities which were used in some of the calculations on DNA–mitomycin complexes. We are grateful to Mr. Eric Petterson of the computer graphics laboratory at the University of California, San Francisco, for his generous help with postscript files of the drug–DNA complexes. Three of us (B.I., T.W., and W.R.) thank Professor Peter Kollman, University of California, San Francisco, for providing a copy of the program AMBER3.0(UCSF).

**Registry No.** GC10, 76957-82-9.

**Supplementary Material Available:** Force field parameters for BMY-25282 (1 page). Ordering information is given on any current masthead page.

# Activity of $N^6$-Substituted 2-Chloroadenosines at $A_1$ and $A_2$ Adenosine Receptors

Robert D. Thompson,[†] Sherrie Secunda,[‡] John W. Daly,[‡] and Ray A. Olsson*[,†,§]

*Departments of Internal Medicine and Biochemistry and Molecular Biology, University of South Florida, Tampa, Florida 33612, and Laboratory of Bioorganic Chemistry, NIDDK, NIH, Bethesda, Maryland 20289.*
*Received May 28, 1991*

Radioligand binding studies of $N^6$-substituted adenosines at the $A_1$ and $A_2$ adenosine receptors of rat brain cortex and rat brain striatum, respectively, show that a 2-chloro substituent does not consistently change the affinity or the selectivity of these analogues for the $A_1$ receptor. A 2-chloro substituent lowers the characteristic stereoselectivity of the $A_1$ receptor toward the *R* diastereomer of $N^6$-(1-phenyl-2-propyl)adenosine. A 2-chloro substituent consistently increases potency of $N^6$-substituted adenosines as agonists at an adenosine $A_2$ receptor stimulatory to adenylate cyclase in PC12 cell membranes.

The ubiquity of $A_1$ and $A_2$ adenosine receptors ($A_1$AR, $A_2$AR) and the several responses that these receptors mediate create side effects that could limit the therapeutic usefulness of this nucleoside. Accordingly, a considerable effort has gone into the synthesis of agonists and antagonists selective for one or the other type of receptor.[1,2] It is now clear that certain $N^6$-alkyl and $N^6$-cycloalkyl substituents promote selectivity for the $A_1$AR[3,4] and certain $N^6$-aralkyl substituents confer potency and selectivity for the $A_2$AR.[5,6] Attempts to improve the potency and selectivity of adenosine by combining modifications in different parts of the molecule have been only partly successful. Whereas an *N*-ethyl 5′-uronamide modification of the ribose increases the potency of adenosine,[7] such a modification of an $N^6$-cycloalkyladenosine has little effect on activity at the $A_1$AR.[8] A 2-chlorosubstituent enhances the potency and selectivity for the $A_1$AR of $N^6$-cyclopentyl-1-deazaadenosine, but not of other $N^6$-substituted 1-deazaadenosines.[9] That discovery led to the development of 2-chloro-$N^6$-cyclopentyladenosine[10] (CCPA), which is more potent at and selective for the $A_1$AR than $N^6$-cyclopentyladenosine (CPA), which until that time was the standard for selective $A_1$AR agonists.[3,11]

Here we report measurements of the affinity for $A_1$AR and $A_2$AR of $N^6$-cyclopentyladenosine, $N^6$-phenyladenosine, and $N^6$-(1-phenyl-2(*R*)-propyl)adenosine ((*R*)-PIA) and its *S* diastereomer ((*S*)-PIA) and comparison of those measurements with the affinities of the corresponding 2-chloroadenosines. In general, our observations do not support the notion that a 2-chloro substituent enhances the potency and selectivity of an $N^6$-substituted adenosine for the $A_1$AR, nor does a 2-chloro substituent appear to enhance the stereoselective recognition of the

Scheme I

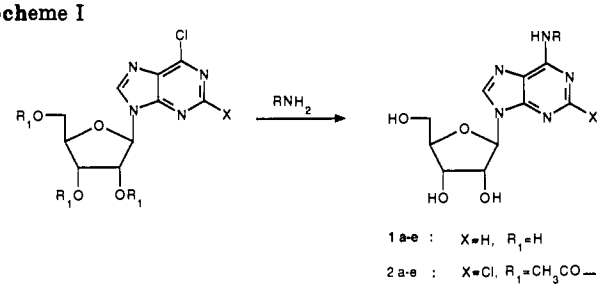


*Address for correspondence: Department of Internal Medicine, Box 19, 12901 Bruce B. Downs Blvd., Tampa, FL 33612.
[†]Department of Internal Medicine.
[‡]Laboratory of Bioorganic Chemistry.
[§]Department of Biochemistry and Molecular Biology.

(1) Jacobson, K. A., Daly, J. W., Manganiello, V., Eds. *Purines in Cellular Signaling. Targets for New Drugs*; Springer-Verlag: New York, 1990.
(2) Williams, M., Ed. *Adenosine and Adenosine Receptors*; Humana: Clifton, N. J., 1990.
(3) Moos, W. S.; Szotek, D. S.; Bruns, R. F. $N^6$-cycloalkyladenosines. Potent $A_1$-selective adenosine agonists. *J. Med. Chem.* **1985**, *28*, 1383–1384.
(4) Daly, J. W.; Padgett, W.; Thompson, R. D.; Kusachi, S.; Bugni, W. J.; Olsson, R. A. Structure–activity relationships for $N^6$-substituted adenosines at a brain $A_1$-adenosine receptor with a comparison to an $A_2$-adenosine receptor regulating coronary blood flow. *Biochem. Pharmacol.* **1986**, *35*, 2467–2481.
(5) Bridges, A. W.; Bruns, R. F.; Ortwine, D. F.; Priebe, S. R.; Szotek, D. S.; Trivedi, B. K. $N^6$-[2-(3,5-dimethoxyphenyl)-2-(2-methylphenyl)ethyl]adenosine and its uronamide derivatives. Novel adenosine agonists with both high affinity and high selectivity for the adenosine $A_2$ receptor. *J. Med. Chem.* **1988**, *31*, 1282–1285.
(6) Kusachi, S.; Thompson, R. D.; Olsson, R. A. Coronary vasoactivity of novel $N^6$-substituted adenosines. *Nucleosides Nucleotides*, in press.
(7) Yeung, S.-M. H.; Green, R. D. [$^3$H]-5′-N-ethylcarboxamido adenosine binds to both $R_a$ and $R_1$ adenosine receptors in rat striatum. *Naunyn-Schmiedeberg's Arch. Pharmacol.* **1984**, *325*, 218–225.

0022-2623/91/1834-3388$02.50/0 